International Journal of Control, Automation and Systems 18(10) (2020) 2630-2640
http://dx.doi.org/10.1007/s12555-018-0895-y
ISSN:1598-6446 eISSN:2005-4092
http://www.springer.com/12555

Liquid Level Tracking Control of Three-tank Systems

Shuyou Yu*, Xinghao Lu, Yu Zhou, Yangyang Feng, Ting Qu, and Hong Chen

Abstract: In this paper, a liquid level tracking controller composed of a feedforward controller and a feedback controller is proposed for three-tank systems. Firstly, the flat property of three-tank systems is verified and a feedforward controller is designed accordingly to track the ideal trajectories. Secondly, in order to eliminate the tracking errors introduced by model uncertainties or unknown disturbances, a nonlinear model predictive controller is designed in which a terminal equality constraint is added for ensuring asymptotic convergence. In addition, an improved cuckoo search algorithm is adopted to solve the optimization problem involved in the nonlinear model predictive control. Finally, the control performance is confirmed by both simulation and experiment results.

Keywords: Cuckoo search algorithm, flat system, liquid level tracking, model predictive control.

1. INTRODUCTION

Liquid level control is important in modern process control since it can potentially improve product quality and enhance economic benefits [1]. Three-tank systems are typical multi-input multi-output (MIMO) systems with the features of strong coupling and nonlinearity, which make it of great research value in the study of liquid level control [2, 3].

Many efforts have been made to solve the liquid level tracking control problem. A neural network based PID controller is proposed in [4], which shows that the standard digital PID controller has faster response and a larger overshoot while the neural network based PID controller can achieve better performance with the price of a relatively slow response. The liquid level control problem of three-tank systems is described as the disturbance attenuation problem of constrained linear systems in [5], which can guarantee both the disturbance attenuation and the time-domain constraint satisfaction.

Nonlinear model predictive control (NMPC) can deal with constraints of MIMO systems [6–9], and can achieve faster response without overshoot compared to PID controller [10–12]. However, its application has been limited due to the heavily computational burden [13, 14]. A model predictive control scheme based on bees algorithm is proposed to reduce the computational burden in [15], however, the computational burden is still too heavy to implement. A RBF-ARX model-based predictive control strategy is proposed to reduce the computational burden by locally linearizing the model at each time instant [16]. But the control accuracy is reduced inevitably due to the model error caused by linearization at each time instant.

In order to enhance the tracking accuracy and avoid the model error caused by linearization, a controller with a feedforward control based on the property of flatness and a model predictive control is proposed in [17]. Through the ideal flat outputs, the ideal state trajectory and control input trajectory can be obtained [18], and the ideal control input could be served as a feedforward in order to achieve fast tracking. A nonlinear model predictive controller of the error system is used as the feedback control to eliminate tracking errors. This two degrees of freedom control structure makes full use of not only the flatness of the system itself, but also the advantages of the NMPC. However, the designed nonlinear model predictive controller is solved using *fmincon* [17], which can only perform one-step prediction in sampling time of 1 second due to the heavily computational burden. It is worth noting that a research has realized multi-step prediction of $T_p = 10$ and achieved good control performance for the three-tank systems using *fmincon* [19]. However, only a simulation rather than an experiment is carried out and its computational time is much longer than 1 second. In order to make multi-step prediction possible in sampling time of 1 second and make the system response smoother, an improved cuckoo search algorithm is proposed in this paper to solve the optimization problem of nonlinear model predictive control.

The rest of this paper is organized as follows: Section 2

Manuscript received December 16, 2018; revised April 28, 2019, September 30, 2019, and January 15, 2020; accepted January 19, 2020. Recommended by Associate Editor Niket Kaisare under the direction of Editor Jay H. Lee. This work was supported by the National Natural Science Foundation of China (No.U1964202, No.61711540307, No.61703176, No.61703178, No.61520106008).

Shuyou Yu, Ting Qu, and Hong Chen are with State Key Laboratory of Automotive Simulation and Control, Jilin University, Changchun 130012, P. R. China (e-mails: {shuyou, quting, chenh}@jlu.edu.cn). Xinghao Lu, Yu Zhou, and Yangyang Feng are with Department of Control Science and Engineering, Jilin University, Changchun 130012, P. R. China (e-mails: {luxh19, zhouyu16, fengyy16}@mails.jlu.edu.cn).
* Corresponding author.

introduces the model of three-tank systems and sets up the control problem. The controller is designed in Section 3. Section 4 describes the application of improved cuckoo search algorithm in constrained optimization problems. Both the simulation and experiment results are shown in Section 5. Some conclusions are drawn in Section 6.

2. PROBLEM SETUP

The first part of this section introduces the nonlinear model of a three-tank systems and the second part describes the control problem.

As shown in Fig. 1, three-tank systems mainly consists of three tanks (Tank 1,Tank 2 and Tank 3) and two pumps (Pump 1 and Pump 2). Pump 1 and Pump 2 absorb liquid from the reservoir and supply liquid respectively to Tank 1 and Tank 2. Tank 3 only gets liquid from Tank 1 and Tank 2 through the connecting pipes between them. The liquid in Tank 2 can inflow to the reservoir through the rightmost pipe. Related parameters are referred in Table 1.

According to the Mass Balance Principle, the three-tank system is described as follows:

$$\begin{cases} S\dot{h}_1 = Q_1 - Q_{13}, \\ S\dot{h}_2 = Q_2 + Q_{32} - Q_{20}, \\ S\dot{h}_3 = Q_{13} - Q_{32}. \end{cases} \tag{1}$$

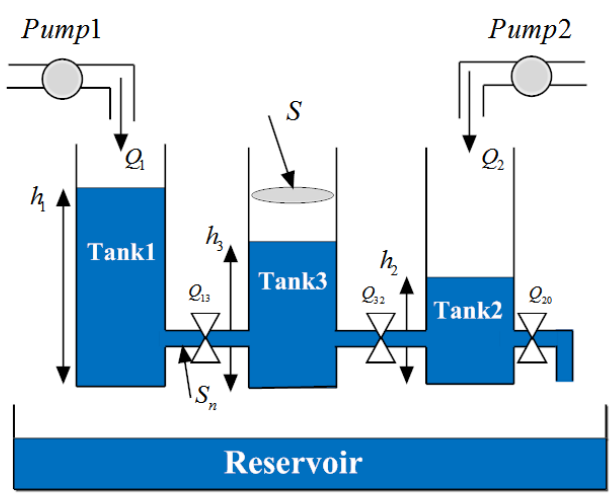

Fig. 1. Sketch of the three-tank systems.

Table 1. Symbols of the three-tank system.

Symbol	Meaning
h_i	liquid level of Tank i $(i = 1,2,3)$
Q_j	flow rate from Pump j to Tank j $(j = 1,2)$
Q_{13}	flow rate from Tank 1 to Tank 3
Q_{32}	flow rate from Tank 3 to Tank 2
Q_{20}	flow rate from Tank 2 to Reservoir
S	cross sectional area of Tank 1,2,3
S_n	cross sectional area of the connecting pipe

In terms of Torricelli Rule, Q_{13}, Q_{32} and Q_{20} are described [3]

$$\begin{cases} Q_{13} = a_{z1} S_n \operatorname{sgn}(h_1 - h_3)(2g|h_1 - h_3|)^{1/2}, \\ Q_{32} = a_{z3} S_n \operatorname{sgn}(h_3 - h_2)(2g|h_3 - h_2|)^{1/2}, \\ Q_{20} = a_{z2} S_n (2gh_2)^{1/2}, \end{cases} \tag{2}$$

where a_{zi} $(i = 1, 2, 3)$ represents the flow coefficient and g represents the gravitational acceleration.

The three-tank system is described as follows according to (1) and (2)

$$\begin{cases} S\dot{h}_1 = Q_1 - a_{z1} S_n \operatorname{sgn}(h_1 - h_3)(2g|h_1 - h_3|)^{1/2}, \\ S\dot{h}_2 = Q_2 + a_{z3} S_n \operatorname{sgn}(h_3 - h_2)(2g|h_3 - h_2|)^{1/2} \\ \qquad - a_{z2} S_n (2gh_2)^{1/2}, \\ S\dot{h}_3 = a_{z1} S_n \operatorname{sgn}(h_1 - h_3)(2g|h_1 - h_3|)^{1/2} \\ \qquad - a_{z3} S_n \operatorname{sgn}(h_3 - h_2)(2g|h_3 - h_2|)^{1/2}. \end{cases} \tag{3}$$

Choose $x = [h_1, h_2, h_3]^T$ as state of the three-tank system and $u = [Q_1, Q_2]^T$ as control input. The state and control input satisfy the following constraints

$$0 \le h_1, h_2, h_3 \le H_{max},$$

and

$$0 \le Q_1, Q_2 \le Q_{max},$$

where H_{max} is the admissible liquid level of three tanks and Q_{max} is the maximum flow that the pumps can provide.

The control objective of the three-tank system is to track the ideal trajectories of h_1 and h_3 by regulation of control input u. At the same time, the state and control input constraints are taken into account.

3. CONTROLLER DESIGN

A controller shown in Fig. 2 is introduced in this section, which includes a feedforward controller and a feedback controller (model predictive control). Denote h_1^* and h_3^* as the ideal trajectories of h_1 and h_3 and assume that h_1^* and h_3^* are finite order continuous. Denote x^f as the ideal trajectories of x obtained from the feedforward controller according to h_1^* and h_3^*, and x_e as the tracking errors coming from the model uncertainties or unknown disturbances. Denote u^f as the feedforward control which can make the system track the ideal trajectories x^f fast and u_e as the feedback control which aims at eliminating the tracking errors x_e.

3.1. Flat systems and feedforward control

The state and input of a flat system can be determined by flat outputs and their finite-order derivatives [18, 21].

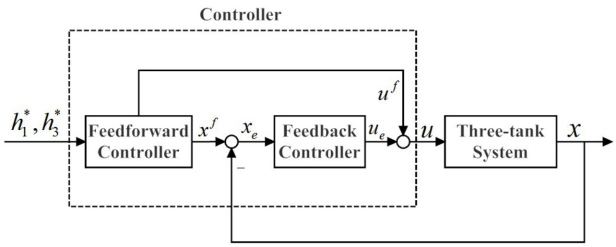

Fig. 2. Control architecture of three-tank systems.

Consider a system $\dot{\tilde{x}} = f(\tilde{x}, \tilde{u})$ with $\tilde{x} \in \Re^n$ and $\tilde{u} \in \Re^m$. If there exists $z = F\left(\tilde{x}, \tilde{u}, \dot{\tilde{u}}, \dots, \tilde{u}^{(l)}\right) \in \Re^m$ such that $\tilde{x} = \alpha(z, \dot{z}, \dots, z^{(p)}), \tilde{u} = \varphi(z, \dot{z}, \dots, z^{(q)})$, then the system is flat and z is called flat outputs. Functions f, F, α and φ and their finite-order derivatives are continuous, and l, p, q are generally not exceeding the system order [20].

Three-tank systems are flat systems and the flat outputs are not unique [22]. Because of the ideal trajectories of h_1 and h_3 are known, h_1 and h_3 can be used as flat outputs, i.e., $z = [h_1, h_3]^T$. In the following, the flat property of three-tank systems will be tested.

According to the system (3), h_2, Q_1 and Q_2 can be expressed as

$$h_2 = h_3 - \frac{1}{2g}\left(\frac{a_{z1}S_n \text{sgn}(h_1 - h_3)\sqrt{2g|h_1 - h_3|} - S\dot{h}_3}{a_{z3}S_n}\right)^2,$$

and

$$\begin{cases} Q_1 = S\dot{h}_1 + a_{z1}S_n \text{sgn}(h_1 - h_3)\sqrt{2g|h_1 - h_3|}, \\ Q_2 = S\dot{h}_2 - a_{z3}S_n \text{sgn}(h_3 - h_2)\sqrt{2g|h_3 - h_2|} \\ \qquad + a_{z2}S_n\sqrt{2gh_2}. \end{cases}$$

Since h_1 and h_3 satisfy the definition of flat outputs, the flat property of the three-tank system is verified. So, the ideal flat outputs can be used to design x^f and u^f. At time instant t, denote the ideal flat outputs as $z^* = [h_1^*(t), h_3^*(t)]^T$ and $x^f(t) = [x_1^f(t), x_2^f(t), x_3^f(t)]^T$, where

$$\begin{cases} x_1^f(t) = h_1^*(t), \\ x_3^f(t) = h_3^*(t), \\ x_2^f(t) = h_3^*(t) - \dfrac{1}{2g}\dfrac{\left(a_{z1}S_n \text{sgn}(\xi)\sqrt{2g|\xi|} - S\dot{h}_3^*(t)\right)^2}{(a_{z3}S_n)^2}, \end{cases} \tag{4}$$

and $\xi = h_1^*(t) - h_3^*(t)$, the feedforward control input is $u^f(t) = [u_1^f(t), u_2^f(t)]^T$ with

$$\begin{aligned} u_1^f(t) =& S\dot{h}_1^*(t) + a_{z1}S_n \text{sgn}(h_1^*(t) - h_3^*(t)) \\ & * \sqrt{2g|h_1^*(t) - h_3^*(t)|}, \\ u_2^f(t) =& S\dot{x}_2^f(t) + a_{z2}S_n\sqrt{2gx_2^f(t)} \\ & - a_{z3}S_n \text{sgn}\left(h_3^*(t) - x_2^f(t)\right)\sqrt{2g\left|h_3^*(t) - x_2^f(t)\right|}. \end{aligned}$$

3.2. Nonlinear model predictive control

Due to model uncertainties, unmodeled dynamics and external disturbances, tracking errors can not be avoided in general. Define $x_e = [x_{e1}, x_{e2}, x_{e3}]^T$ as state of the error system and $u_e = [u_{e1}, u_{e2}]^T$ as control input, where

$$\begin{cases} x_{e1} = x_1^f - h_1, \\ x_{e2} = x_2^f - h_2, \\ x_{e3} = x_3^f - h_3, \\ u_{e1} = Q_1 - u_1^f, \\ u_{e2} = Q_2 - u_2^f. \end{cases} \tag{5}$$

The error system can be described as

$$\begin{cases} \dot{x}_{e1} = \dot{x}_1^f - \dot{h}_1, \\ \dot{x}_{e2} = \dot{x}_2^f - \dot{h}_2, \\ \dot{x}_{e3} = \dot{x}_3^f - \dot{h}_3, \end{cases} \tag{6}$$

where $\dot{h}_1, \dot{h}_2$ and $\dot{h}_3$ can be expressed according to (3) and (5)

$$\begin{cases} \dot{h}_1 = \frac{u_{e1} + u_1^f}{S} - \frac{a_{z1}S_n}{S}\left(2g\left(x_{e1} - x_{e3} + x_1^f - x_3^f\right)\right)^{1/2}, \\ \dot{h}_2 = \frac{u_{e2} + u_2^f}{S} + \frac{a_{z3}S_n}{S}\left(2g\left(x_{e3} - x_{e2} + x_3^f - x_2^f\right)\right)^{1/2}, \\ \qquad - \frac{a_{z2}S_n}{S}\left(2g\left(x_{e2} + x_2^f\right)\right)^{1/2}, \\ \dot{h}_3 = \frac{a_{z1}S_n}{S}\left(2g\left(x_{e1} - x_{e3} + x_1^f - x_3^f\right)\right)^{1/2} - \frac{a_{z3}S_n}{S} \\ \qquad * \left(2g\left(x_{e3} - x_{e2} + x_3^f - x_2^f\right)\right)^{1/2}, \end{cases} \tag{7}$$

and $\dot{x}_1^f, \dot{x}_2^f$ and $\dot{x}_3^f$ can be expressed according to (4)

$$\begin{cases} \dot{x}_1^f = \dot{h}_1^*, \\ \dot{x}_3^f = \dot{h}_3^*, \\ \dot{x}_2^f = \dot{h}_3^* - \dfrac{1}{2g(a_{z3}S_n)^2} \\ \qquad * \left(a_{z1}S_n \text{sgn}\left(h_1^* - h_3^*\right)\sqrt{2g\left|h_1^* - h_3^*\right|} - S\ddot{h}_3^*\right)^2. \end{cases} \tag{8}$$

Combining (7) and (8), the error system (6) is written in the following form

$$\dot{x}_e = f_e(x_e, u_e),$$

where the function f_e is parameter-dependent on the ideal flat outputs and their finite-order derivatives. The function

$f_e(x_e, u_e)$=0 while $x_e = [0,0,0]^T$ and $u_e = [0,0]^T$. That is to say, $[0,0,0]^T$ is the equilibrium of the error system (6).

In order to make the tracking errors converge to zero in the framework of model predictive control [23, 24], the following online optimization problem is solved at each time instant t.

Problem 1:

$$\begin{aligned}&\dot{\bar{x}}_e(\tau) = f_e(\bar{x}_e(\tau), \bar{u}_e(\tau)),\\&\bar{u}_{er}(\tau) + u_r^f(\tau) \in [0, Q_{\max}],\ r = 1,2\\&x_q^f(\tau) - \bar{x}_{eq}(\tau) \in [0, H_{max}],\ q = 1,2,3,\ t \le \tau \le t + T_p,\\&\bar{x}_e(t) = x_e(t),\\&\bar{x}_e(t+T_p) = 0,\end{aligned}$$

with $J(x_e(t), U_t) = \int_t^{t+T_p}\left(||\bar{x}_e(\tau)||_Q^2 + ||\bar{u}_e(\tau)||_R^2\right)d\tau$.

In Problem 1, $x_e(t)$ is the error state at time instant t, $U_t := u_e(\cdot, x_e(t))$ denotes the control input trajectory related to $x_e(t)$. $\bar{u}_e(\tau)$ is the predicted control input for all $\tau \in [t, t+T_p]$ and $\bar{u}_e(\tau) = u_e(\tau, x_e(t))$. Both Q and R are positive definite weighting matrices with appropriate dimensions, T_p is the prediction horizon. Problem 1 is solved in discrete time with a sampling of δ.

Denote U_t^* as the optimal solution of Problem 1, i.e., $U_t^* = u_e^*(\cdot, x_e(t))$, then the control input $u_e(\tau)$ of nonlinear model predictive control is

$$u_e(\tau) = u_e^*(\tau, x_e(t)),\quad \tau \in [t, t+\delta].$$

So, the actual control input implementing to the three-tank systems is

$$u(\tau) = u^f(\tau) + u_e(\tau),\quad \tau \in [t, t+\delta].$$

Remark 1: Due to the terminal equality constraint of $\bar{x}_e(t+T_p) = 0$ in Problem 1, both recursive feasibility of Problem 1 and asymptotic trajectory tracking can be guaranteed [25].

Remark 2: Terminal equality constraints rather than terminal inequality constraints is considered in this paper since path tracking rather than a regulation problem is considered and three-tank systems are strong nonlinear.

4. SOLUTION OF CONSTRAINED OPTIMIZATION PROBLEM

A general constraint optimization problem can be described in the following form

$$\begin{aligned}&\min \phi(\theta)\\&\text{s.t.} \begin{cases} g_i(\theta) \le 0, i \in \{1,2,\ldots,q_c\},\\ h_j(\theta) = 0, j \in \{q_c+1,\ldots,l_c\},\end{cases}\end{aligned} \tag{9}$$

where $\phi(\theta)$ is the objective function of the constrained optimization problem, θ is the optimization variable, $g_i(\theta)$ and $h_j(\theta)$ are the inequality constraint and equality constraint that need to be satisfied respectively, q_c is the number of inequality constraints, $l_c - q_c$ is the number of equality constraints.

4.1. Basic cuckoo search algorithm

Cuckoo search algorithm (CSA) was first proposed by Yang and Deb in 2009 as a new type of swarm intelligence optimization algorithm [26]. Compared with other swarm intelligence optimization algorithms, such as artificial bee colony algorithm and particle swarm optimization algorithm, CSA has better global search capability. It has been successfully applied to image processing, deep learning, data mining and other optimization problems.

The cuckoo search algorithm is derived from the unique nesting and spawning behavior of cuckoos. In the cuckoo search algorithm, the host bird nest selected by the cuckoo represents a solution to the optimization problem. The essence of the algorithm is to replace the poorer solutions of the previous generation with new and better solutions. After the succession of multiple generations of populations, the highest evaluated nest position is retained as the optimal solution. In order to simulate and simplify the cuckoo's nesting and spawning behavior, three ideal rules are assumed:

1) Each cuckoo produces only one egg at a time, and the choice of the host nest follows a random selection;
2) The best nest remains to the next generation;
3) The number of host nests is fixed as $n \in N$, and the probability that the eggs hatched by the cuckoos and found by the host belongs to $p_a \in [0,1]$.

Based on the above three rules, a new solutions x_i^{t+1} generated by the basic cuckoo search algorithm is

$$x_v^{t+1} = x_v^t + \eta \oplus L\acute{e}vy(\beta),\quad v = 1,2,\ldots,n,$$

where the product $\oplus$ means entry-wise multiplications, η is the search step size, n is the number of host nests, t is the number of iteration, $L\acute{e}vy(\beta)$ is a random search path following the *Lévy* distribution with

$$L\acute{e}vy = t^{-\beta},\quad \beta \in (0,3].$$

Remark 3: In general, nonlinear programming problem such as Problem 1 can be solved by Interior Point Optimizer (IPOPT) as well [27], which implements an interior point line search filter method aiming to find a local solution, while CSA has better global search capability.

4.2. Improved cuckoo search algorithm

The larger the search step size of the cuckoo algorithm, the stronger the global search ability of the algorithm. The search step is improved by [28]

$$\eta = 0.001 \times t_{\max} \times e^{(-(t/t_{\max}))}$$

where $t_{\max}$ is maximum number of iterations. This improved method decreases the search step size with the increase of the number of iterations, i.e.. decreases the search step size faster in the early stage, and decreases the search step size gradually. The large step search in the early stage is beneficial to enhance the global search ability of the algorithm, and the decrease of the search step size is beneficial to improve the local search accuracy and greatly improve the search performance of the algorithm.

In addition, according to the idea of the simplex method, before the succession of the next generation cuckoo population, select some poor bird nest positions in the population, and generate new bird nests [29], then use them as the next generation. The specific implementation is as follows: assume that x_s is the initial position of a currently selected bird's nest, x^* is the current optimal bird's nest location, x_* is the current sub-optimal bird's nest location, $f(x_s)$, $f(x^*)$ and $f(x_*)$ are the corresponding fitness values. x_m is the midpoint of x^* and x_*, that is $x_m = (x^* + x_*)/2$. Produce a reflection point x_r with $x_r = x_m + (x_m - x_s)$, and denote $f(x_r)$ as the corresponding fitness value. Three cases are considered:

1) $f(x_r) \le f(x^*)$
   Generate $x_a = x_m + 2(x_r - x_m)$. If $f(x_a) < f(x_r)$, replace x_s with x_a; otherwise replace with x_r.
2) $f(x_r) \ge f(x_s)$
   Generate $x_b = x_m + 0.5(x_s - x_m)$. If $f(x_b) < f(x_s)$, replace x_s with x_b.
3) $f(x_s) < f(x_r) < f(x^*)$
   Generate $x_c = x_m - 0.5(x_s - x_m)$ If $f(x_c) < f(x_r)$, replace x_s with x_c; otherwise replace with x_r.

The generation process is shown in Fig. 3.

Similar to the particle swarm optimization algorithm, the cuckoo search algorithm is difficult to deal with the constraints of the optimization problem, and the phenomenon of jumping out of the search boundary may occur during the search process. For this kind of cross-border behavior, the cross-border bird nest is forcibly set on the search boundary usually. Although the search result is guaranteed to be within the boundary constraint, it is inevitable to lose some of the bird's nest search vitality. The constraint optimization problem is transformed into an unconstrained optimization problem by penalty function methods, thus the out-of-bound problem of the cuckoo search algorithm is avoided.

Choose the penalty function of the following form [31]

$$G(x) = f(x) + C(\rho) \times \varphi(x),$$

where $C(\rho)$ is the penalty factor, ρ is the ratio of the feasible solution. The penalty factor $C(\rho) := e^{\alpha_0(1-\rho)} - 1$ decreases if ρ increases, where $\alpha_0 > 0$ is an adjustable parameter. The penalty term $\varphi(x)$ represents the degree

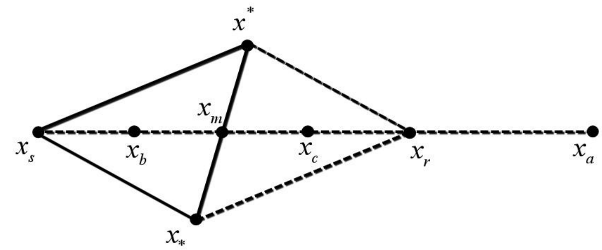

Fig. 3. Generation of a new bird's nest position in simple bird method.

Algorithm 1: Improved cuckoo search algorithm.

1: Set initial population U^t and find the optimal nest location x_b^t;
2: **while** $(t \le t_{max})$ **do**
3: Reserve x_b^t and update population U^t;
4: Random elimination of U^t according to probability p_e;
5: Improve the poor elements of U^t according to the simplex method;
6: Set $t = t + 1$;
7: **end while**
8: Output x_b^t;

which variables to be optimized violate the constraint conditions, and $\varphi(x) = \sum_{j=1}^{l} \varphi_j(x)$ with

$$\varphi_j(x) = \begin{cases} \max\{0, g_j(x)\}, & 1 \le j \le q; \\ \max\{0, |h_j(x)| - \varepsilon\}, & q+1 \le j \le l. \end{cases}$$

The improved cuckoo search algorithm is Algorithm 1.

Remark 4: The improved cuckoo search algorithm is generic in many areas of optimization and computational intelligence with promising efficiency. For example, in the engineering design applications, cuckoo search has superior performance over other algorithms for a range of continuous optimization problems such as spring design and welded beam design problems [30].

4.3. Solution to constrained optimization problem based on improved cuckoo search algorithm

Rewrite Problem 1 into the form of (9), and solve it by the improved cuckoo algorithm. The proposed control law can be formally obtained by Algorithm 2.

5. SIMULATION AND EXPERIMENT

In this section, simulation and experiment are carried out separately for the three-tank system, which operated on Intel(R) Core(TM) i7-4790 CPU (3.6GHz).

Algorithm 2: Liquid level tracking of three-tank systems.

while $(t \leq 1500)$ **do**
  Calculate $x^f(t)$ and $u^f(t)$ via (8)-(9) at time instant t ;
  Measure system state $x(t)$ at time instant t;
  Calculate the state $x_e(t)$ via (10);
  Solve Problem 1 to get $u_e(t)$ via (23);
  Take the value $u(t)$ calculated via (17) as the current control input of the system until the next sampling time $t+\delta$;
  At time $t+\delta$, set $t := t+\delta$;
end while

Table 2. Parameters of three-tank systems.

Symbol	Parameters
R	diag$\{1,1\}$
Q	diag$\{100, 200, 1000\}$
T_p	5 s
Q_{max}	130 ml/s
H_{max}	60 cm
S	154 cm^2
S_n	0.5 cm^2
g	9.8 m/s^2
a_{z1}	0.3162
a_{z2}	0.7121
a_{z3}	0.5130

5.1. Case 1: Fixed point tracking

The ideal trajectories are $h_1^* = 25$ cm and $h_3^* = 14.2$ cm. Accordingly, $h_2^* = 10$ cm. The sampling time of $\delta = 0.5$ s. Other related parameters of the system and controller are listed in Table 2. The simulation results are shown in Figs. 4-7 and the experiment results are shown in Figs.8-9, respectively. Note that, compared with $T_\text{p} = 1$ s in [17], $T_\text{p} = 5$ s is set in this paper.

As can be seen from Fig. 4, compared with [3] which linearized the system around the equilibrium point, the controller designed in this paper has no overshoot when tracking fixed points. According to Fig. 5, the control input constraints are satisfied. As shown in Fig. 6, the maximum computational time does not exceed 0.5 seconds which meets the experimental requirements. As can be seen from Fig. 7, the value function shows a decreasing monotonic trend.

Figs. 8 and 9 are corresponding experimental results. As can be seen from Fig. 8, the experimental results are consistent with the simulation results and have obvious advantages over the results in [3]. It can be seen from the evolution of control input shown in Fig. 9 that in the initial stage, when the actual liquid level is far from the ideal level, the pump flow remains at the maximum limit value of 130, which makes the tank level rise rapidly and the

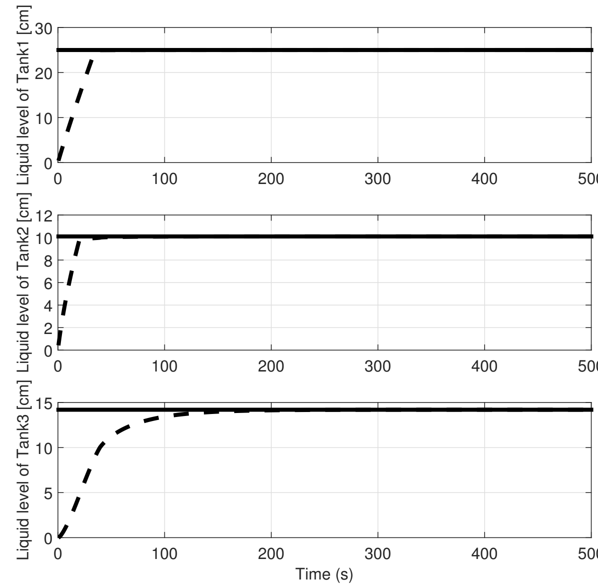

Fig. 4. The liquid level in simulation (Case 1).

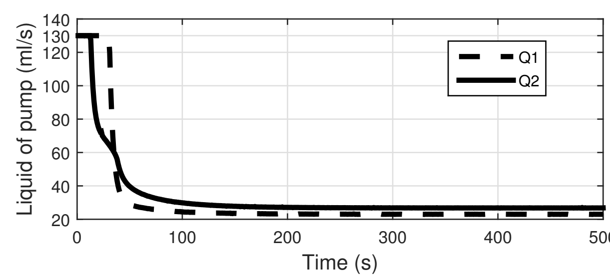

Fig. 5. The control inputs in simulation (Case 1).

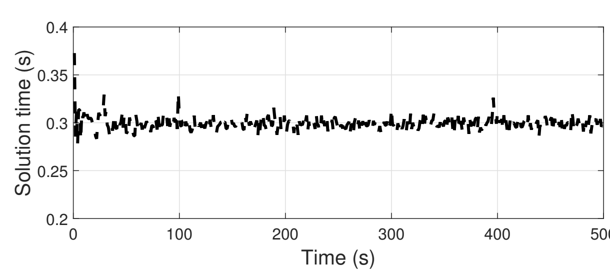

Fig. 6. The computational time in simulation (Case 1).

control input constraints are well satisfied. When the actual liquid level is gradually close to the ideal level, the pump flow also gradually decreases; when the actual liquid level tracks the ideal liquid level, the flow of the pump fluctuates frequently in the equilibrium point due to the fluctuation of the water tank level and the existence of measurement noises and model errors.

Fig. 10 is corresponding simulation results solved by *fmincon*, in which the mean square error of h_1, h_2, h_3 are 13.5270 cm^2, 1.1934 cm^2, 8.5023 cm^2 respectively

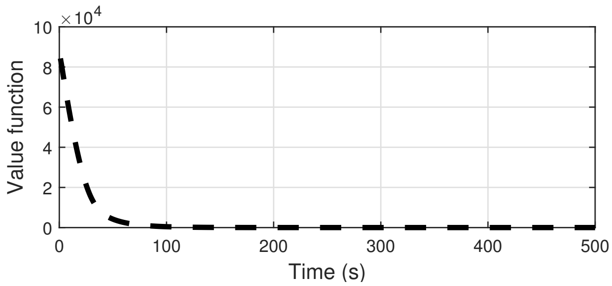

Fig. 7. The value function in simulation (Case 1).

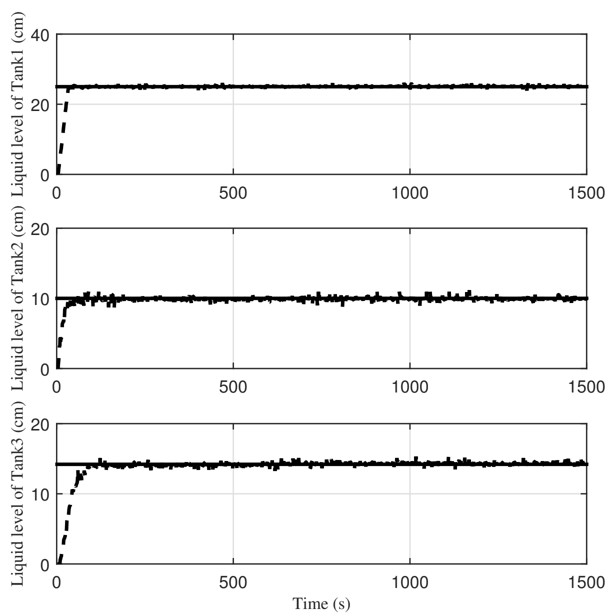

Fig. 8. The liquid level in experiment (Case 1).

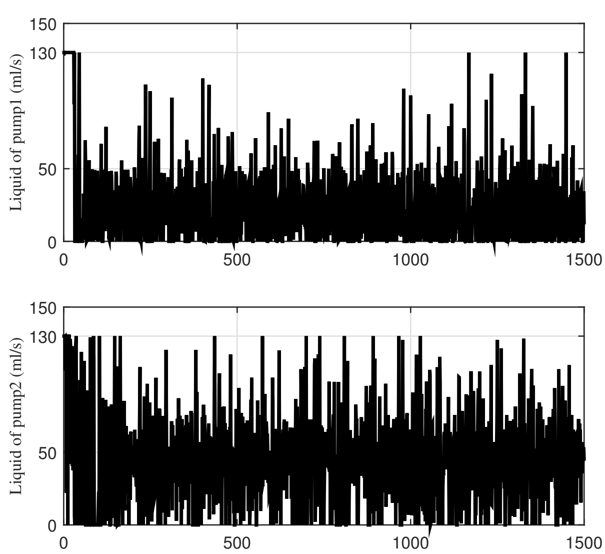

Fig. 9. The control inputs in experiment (Case 1).

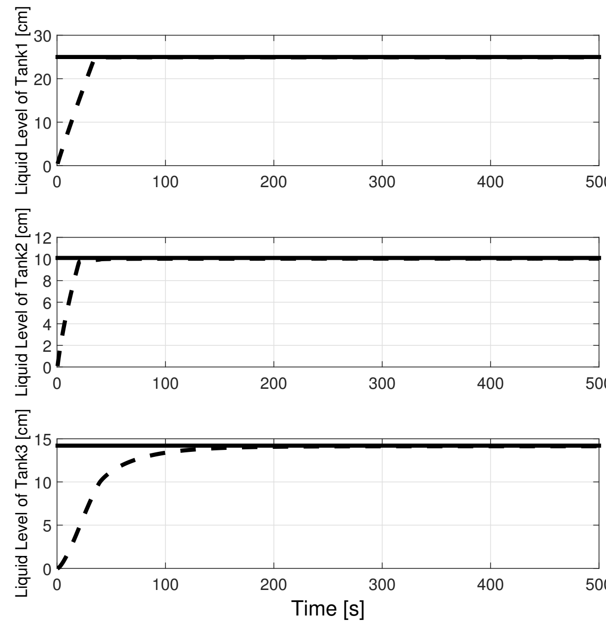

Fig. 10. The liquid level in simulation by fmincon.

Table 3. Comparison with [19].

	work in [19]	work here
control problem	regulation & servo	regulation & tracking
convergence guaranteed	no	yes
simulation or experiment	simulation	simulation & experiment
computational time per iteration	59.05 s	within 0.45 s

and the steady-state error of h_1, h_2, h_3 are 0.0706 cm, 0.0624 cm, 0.0647 cm, respectively; however in Fig. 4, the mean square error of h_1, h_2, h_3 are 13.5138 cm^2, 1.1062 cm^2, 8.3883 cm^2, respectively and the steady-state error of h_1, h_2, h_3 are 0.0001 cm, 0.0001 cm, 0.0001 cm, respectively, which shows the improved cuckoo algorithm has the better control performance.

Remark 5: Multi-step prediction of NMPC for the three-tank systems is implemented in [19] as well. A detailed comparison can be found in Table 3.

5.2. Case 2: Curve tracking

The ideal trajectories are

$$h_1^*(t) = 8\sin(\pi t/500 + 3/2\pi) + 25, \quad t \in (0, 1500]$$
$$h_3^*(t) = 8\sin(\pi t/500 + 3/2\pi) + 15, \quad t \in (0, 1500].$$

The simulation results are shown in Figs. 11-15 and the experiment results are shown in Figs. 16-18, respectively. It can be seen from Fig. 11 that the actual liquid level of the three water tanks can track the ideal liquid level.

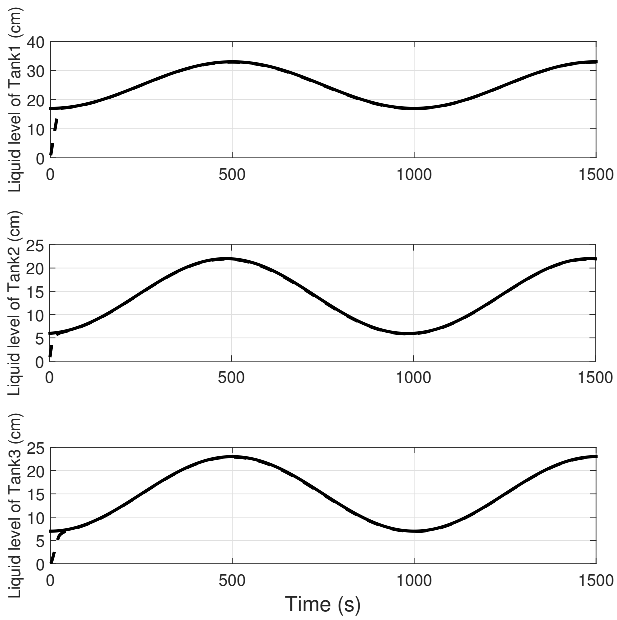

Fig. 11. The liquid level in simulation (Case 2).

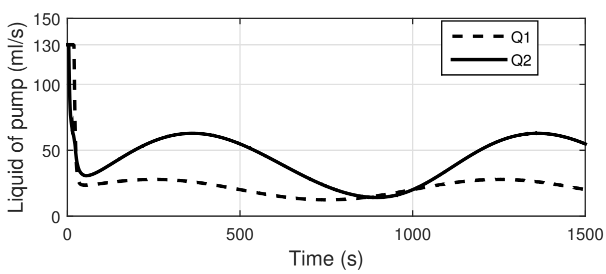

Fig. 12. The control inputs in simulation (Case 2).

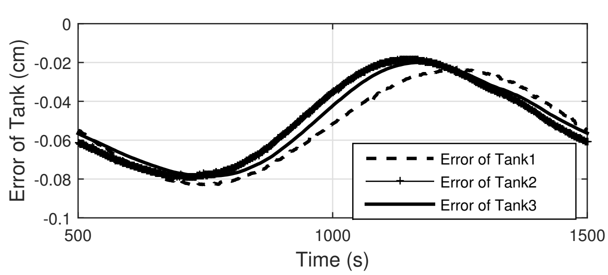

Fig. 13. Tracking errors in simulation (Case 2).

Fig. 18 is the evolution of control input, which meets the control input constraints. Fig. 17 shows the tracking error of three tanks after 500 seconds. It can be seen that the tracking error is within 0.15 cm. Fig. 14 shows that the cost function is monotonically decreasing with time goes by. As can be seen from Fig. 15, the maximum computational time does not exceed 0.45 seconds. At the initial time instant, both tracking errors and control inputs are large due to the large differences between the real states and the ideal states. After about 250 seconds, the tracking

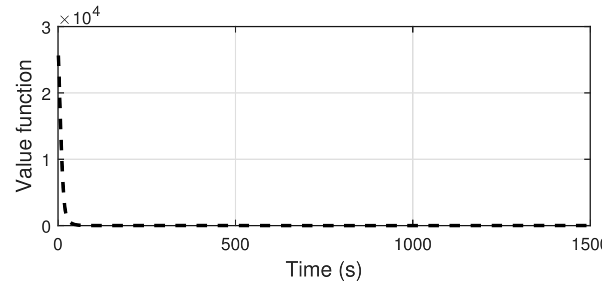

Fig. 14. The value function in simulation (Case 2).

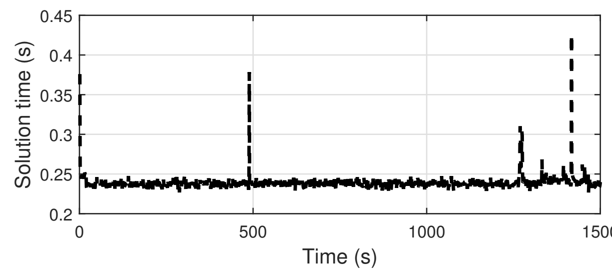

Fig. 15. The computational time in simulation (Case 2).

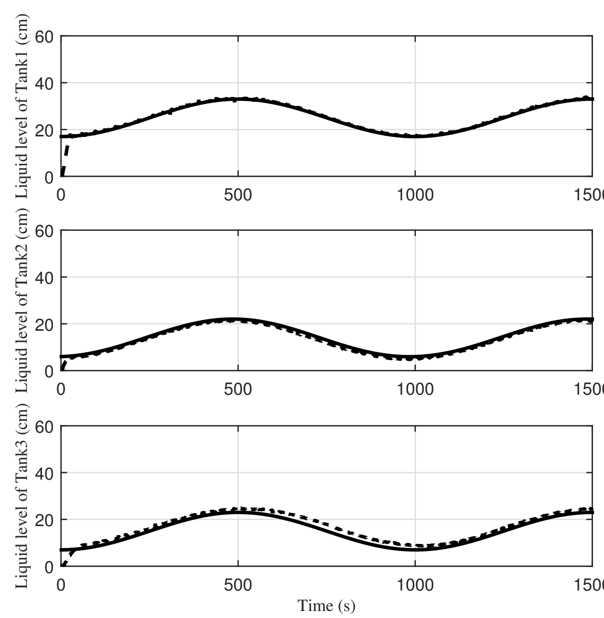

Fig. 16. The liquid level in experiment (Case 2).

errors are kept within 0.2 cm. Accordingly, the control inputs vary smoothly. So, the proposed scheme can track the ideal trajectories with high accuracy.

Compared with simulation results, an experiment with the same parameters as simulation achieves the similar results, c.f., Figs. 16-18. But, the tracking errors are larger than the results in simulation due to the existence of model errors and large measurement noises. In addition, fluctuation of measurement noises leads to the fluctuation of the

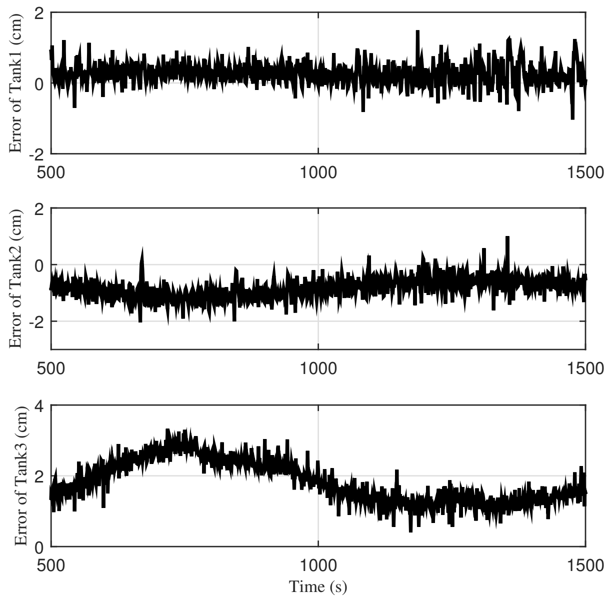

Fig. 17. Tracking errors in experiment (Case 2).

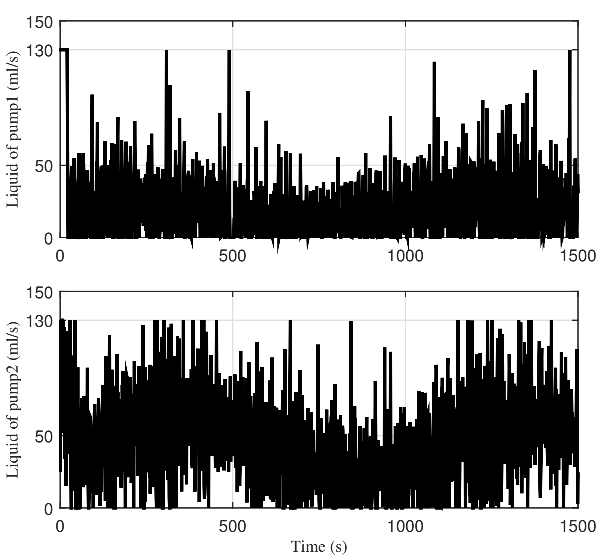

Fig. 18. The control inputs in experiment (Case 2).

pumps, shown in Fig. 18. After about 250 seconds, the tracking errors are kept within 3cm shown in Fig. 17. Although the measurement noises are large to some extent, the proposed scheme can still track the ideal trajectories in a satisfied way.

6. CONCLUSION

A practical liquid level tracking control method was proposed in this paper, in which a feedforward controller was obtained utilizing the flatness property of three tank systems. Model predictive control, a feedback control method, kept the system dynamics in a small area around the trajectory. Compared with the schemes which linearized the system around the trajectory, the proposed scheme can achieve high accuracy and deal with state and input constraints directly. Furthermore, an improved cuckoo optimization algorithm was proposed to solve the involved optimization problem. Future research will focus on reducing influences of measurement noises or model mismatches which lead to large errors in the experiment.

REFERENCES

[1] D. Chirita, A. Florescu, B. C. Florea, R. Ene, and D. A. Stoichescu, "Liquid level control for industrial three tanks system based on sliding mode control," *Revue Roumaine Des Sciences Techniques-Serie Electrotechnique Et Energetique*, vol. 60, no. 4, pp. 437-446, 2015.

[2] Z. Shi, *Three Tank Water Level Control Based on Predictive Control Algorithm*, Shenyang Ligong University, 2013.

[3] Y. Wang, *Liquid Level Control of a Three-tank System*, Jilin University, 2017.

[4] S. Ge and J. Lu, "Neural network PID control of three-tank system based on decoupling," *Journal of Hunan University of Technology*, 2008.

[5] S. Yu, H. Chen, P. Zhang, R. Sun, and M. Shi, "Moving horizon H_∞ control of a three-tank system and its experiment study," *Journal of Northeastern University (Natural Science)*, vol. 28, pp. 82-91, 2007.

[6] H. Chen, S. Yu, X. Lu, F.Xu, T. Qu, and F. Wang, "Applying model predictive control in automotive," *Proc. of the 10th World Congress on Intelligent Control and Automation*, 2012.

[7] R. Yu, H. Guo, Z. Sun, and H. Chen, "MPC-based regional path tracking controller design for autonomous ground vehicles," *Proc. of IEEE International Conference on Systems, Man, and Cybernetics*, IEEE, pp. 2510-2515, 2016.

[8] M. Yue, C. An, and J. Z. Sun, "An efficient model predictive control for trajectory tracking of wheeled inverted pendulum vehicles with various physical constraints," *International Journal of Control, Automation and Systems*, vol. 16, no. 1, pp. 265-274, 2018.

[9] F. Deng, H. L. Yang, and L. J. Wang, "UKF based nonlinear offset-free model predictive control for ship dynamic positioning under stochastic disturbances," *International Journal of Control, Automation and Systems*, vol. 17, no. 12, pp. 3079-3090, 2019.

[10] F. Salem and M. I. Mosaad, "A comparison between MPC and optimal PID controllers: case studies," *Michael Faraday IET International Summit*, 2015.

[11] N. Parikh, S. Rathore, R. Misra, and A.Markana, "A comparison between NMPC and LQG for the level control of three tank interacting system," *Proc. of Indian Control Conference (ICC)*, pp. 200-205, 2017.

[12] A. Bamimore, O. Taiwo, and R. King, "Comparison of two nonlinear model predictive control methods and implementation on a laboratory three tank system," *Proc. of 50th IEEE Conference on Decision and Control and European Control Conference (CDC-ECC)*, pp. 5242-5247, 2011.

[13] J. Zhang, X. Cheng, and J. Zhu, "Control of a laboratory 3-DOF helicopter: explicit model predictive approach," *International Journal of Control, Automation and Systems*, vol. 14, no. 2, pp. 389-399, 2016.

[14] S. M. Tabatabaei, S. Kamali, and M. R. Jahed-Motlagh, "Practical explicit model predictive control for a class of noise-embedded chaotic hybrid systems," *International Journal of Control, Automation and Systems*, vol. 17, no. 4, pp. 857-866, 2019.

[15] M. Sarailoo, Z. Rahmani, and B. Rezaie, "A novel model predictive control scheme based on bees algorithm in a class of nonlinear systems: application to a three tank system," *Neurocomputing*, vol. 152, pp. 294-304, 2015.

[16] F. Zhou, H. Peng, Y. Qin, X. Zeng, W. Xie, and J. Wu, "RBF-ARX model-based MPC strategies with application to a water tank system," *Journal of Process Control*, vol. 34, pp. 97-116, 2015.

[17] S. Yu, Y. Zhou, Y. Feng, T. Qu, and H. Chen, "Liquid level tracking control of three-tank systems," *Proc. of 37th Chinese Control Conference (CCC)*, pp. 3541-3545, 2018.

[18] M. Fliess, J. Lévine, and P. Martin, "Flatness and defect of nonlinear systems: introductory theory and examples," *International Journal of Control*, vol. 61, no. 6, pp. 1327-1361, 1995.

[19] J. Prakash, S. C. Patwardhan, and S. L. Shah, "State estimation and nonlinear predictive control of autonomous hybrid system using derivative free state estimators," *Journal of Process Control*, vol. 20, no. 7, pp. 787-799, 2010.

[20] C. M. Torres, L. Lavigne, and F. Cazaurang, "Fault detection and isolation on a three tank system using differential flatness," *Proc. of Control Conference*, 2013.

[21] R. M. Murray, "Trajectory generation for a towed cable system using differential flatness," *Proc. of IFAC World Congress*, pp. 395-400, 1996.

[22] C. M. Torres, L. Lavigne, F. Cazaurang, E. A. Garcia, and D. D. Romero, "Fault tolerant control of a three tank system: a flatness based approach," *IEEE Control and Fault-Tolerant Systems*, pp. 529-534, 2014.

[23] Y. Liu, S. Yu, Y. Guo, B. Gao, and H. Chen, "Receding horizon control for path following problems of wheeled mobile robots," *Control Theory and Applications*, vol. 34, no. 4, pp. 424-432, 2017.

[24] S. Yu, X. Li, H. Chen, and F. Allgöwer, "Nonlinear model predictive control for path following problems," *International Journal of Robust and Nonlinear Control*, vol. 25, no. 8, pp. 1168-1182, 2015.

[25] J. B. Rawlings and D. Q. Mayne, *Model Predictive Control: Theory and Design*, Nob Hill Pub., Madison, Wisconsin, 2009.

[26] X. S. Yang and S. Deb, "Engineering optimisation by cuckoo search," *International Journal of Mathematical Modelling & Numerical Optimisation*, vol. 1, no. 4, pp. 330-343, 2010.

[27] L. T. Biegler and V. M. Zavala, "Large-scale nonlinear programming using IPOPT: an integrating framework for enterprise-wide dynamic optimization," *Computers & Chemical Engineering*, vol. 33, no. 3, pp. 575-582, 2009.

[28] L. I. Rong-Yu and D. Rui-Wen, *Adaptive Step-size Cuckoo Search Algorithm*, Computer Science, 2017.

[29] X. Zhen, *Research and Application of Bat Algorithm Based on Levy Flight and Simplex Method*, Guangdong University of Technology, 2016.

[30] X. S. Yang and S. Deb, "Cuckoo search: recent advances and applications," *Neural Computing and Applications*, vol. 24, no. 1, pp. 169-174, 2014.

[31] H. L. Cai, *Research and Application of Penalty Function Method in Constrained Optimization*, East China Normal University, 2015.

Shuyou Yu received his B.S. and M.S. degrees in control science and engineering from Jilin University, China, in 1997 and 2005, respectively, and a Ph.D. degree in engineering cybernetics from the University of Stuttgart, Germany, in 2011. From 2010 to 2011, he was a Research and Teaching Assistant with the Institute for Systems Theory and Automatic Control, University of Stuttgart. In 2012, he joined the Department of Control Science and Engineering, Jilin University, as a Faculty Member, where he is currently a Full Professor. His main research interests include model predictive control, robust control, and its applications in mechatronic systems.

Xinghao Lu received his B.E. degree from the College of Communication Engineering, Jilin University, in 2019. He is currently pursuing a master's degree with the Department of Control Science and Engineering, Jilin University. His research interests include model predictive control and machine learning.

Yu Zhou received her B.E. degree from the Jilin Jianzhu University, China, in 2016, and an M.S. degree in control science and engineering from Jilin University, China, in 2019. During the master's degree, she mainly studied nonlinear control strategies of three-tank systems.

Yangyang Feng received his B.E. degree from the Jilin Agricultural University, China, in 2016, and an M.S. degree in the control science and engineering from Jilin University, China, in 2019. He is currently pursuing a Ph.D. degree with the Department of Control Science and Engineering, Jilin University, China. His research interests include nonlinear control, adaptive control, and system identification.

Ting Qu received her B.S. and M.S. degrees from the Northeast Normal University, Changchun, China, in 2006 and 2008, respectively, and a Ph.D. in control science and engineering from the Jilin University of China in 2015. Since 2015, she is a lecturer with the State Key Laboratory of Automotive Simulation and Control at the Jilin University, China. Her research interests include model predictive control and driver modeling.

Hong Chen received her B.S. and M.S. degrees in process control from Zhejiang University, Zhejiang, China, in 1983 and 1986, respectively, and a Ph.D. degree in system dynamics and control engineering from the University of Stuttgart, Stuttgart, Germany, in 1997. Since 1999, she has been a professor at Jilin University, Changchun, China, where she currently serves as Tang Aoqing Professor and as the director of the State Key Laboratory of Automotive Simulation and Control. Her current research interests include model predictive control, optimal and robust control, nonlinear control and applications in mechatronic systems focusing on automotive systems.